The Belle II Experiment

J. Kahn (on behalf of the Belle II Collaboration)
Ludwig Maximilians University, Munich, Germany

Abstract
Set to begin data taking at the end of 2018, the Belle II experiment is the next-generation B-factory experiment hosted at KEK in Tsukuba, Japan. The experiment represents the cumulative effort from the collaboration of experimental and detector physics, computing, and software development. Taking everything learned from the previous Belle experiment, which ran from 1998 to 2010, Belle II aims to probe deeper than ever before into the field of heavy quark physics. By achieving an integrated luminosity of 50 ab^{-1} and accumulating 50 times more data than the previous experiment across its lifetime, along with a rewritten analysis framework, the Belle II experiment will push the high precision frontier of high energy physics. This paper will give an overview of the key components and development activities that make the Belle II experiment possible.

Keywords
Belle II; SuperKEKB; B physics.

1 Introduction

The Belle II experiment is a detector based high energy physics experiment designed to make precision measurements of heavy quark and lepton physics processes. The experiment has two key components: the SuperKEKB e^+e^- collider which will produce a large volume of B meson pairs, and the Belle II detector which will record the products of the decays of the B mesons. The Belle II collaboration was formed in 2009 with the aim of taking everything learned from the predecessor Belle experiment and using it to build a high statistics B physics factory detector that would be sensitive enough to probe for New Physics (NP). The goal was for the detector to achieve a performance similar to or better than that of the Belle detector in the harsher beam background environment produced by the upgraded SuperKEKB collider. There was already a decade–long history of success at e^+e^- colliders from not only Belle, but also its companion experiment BaBar. Most notably for Belle was the confirmation of the Kobayashi–Maskawa–mechanism with the charge–parity (CP) asymmetries in the decays of b–quarks which led to the Nobel prize being awarded to Kobayashi and Maskawa in 2008 [1]. Other great achievements in flavour physics including measurements of unitarity triangle angles, time–dependent CP violation (CPV), new resonances [2], etc., are summarised nicely in Ref. [3]. The Belle collaboration is currently sustaining ~ 20 publications a year with further analyses ongoing. The latest hint of new physics to come out of these ongoing analyses is from the measurement of the ratio $R(D^{(*)}) = \frac{\bar{B}^0 \to D^{*+}\tau^-\bar{\nu}_\tau}{\bar{B}^0 \to D^{*+}\ell^-\bar{\nu}_\ell}$ $(\ell = e, \mu)$ using semi–leptonic tagging [4]. When averaged with BaBar and LHCb they show a 4.0σ disagreement with Standard Model (SM) predictions, as seen in Fig. 1 [5].

With the 50 ab^{-1} of data expected to be collected at Belle II the hope is to give insight into some of the big questions that plague the SM. One of these being to look for new sources of CPV, as the SM does not provide enough to explain the matter–antimatter asymmetry we see in the universe today. In addition, NP searches in semi–leptonic and leptonic decays can be performed, along with investigations of other NP areas such as lepton flavour violation, dark sector, etc. More details on NP opportunities at Belle II can be seen in Ref. [6], and the theoretical prospects for B physics are discussed in Ref. [7].

There are several unique experimental advantages to using a B–factory as opposed to measuring B decays from a hadron collider as is done at LHCb. Most prominently the environment is exceptionally
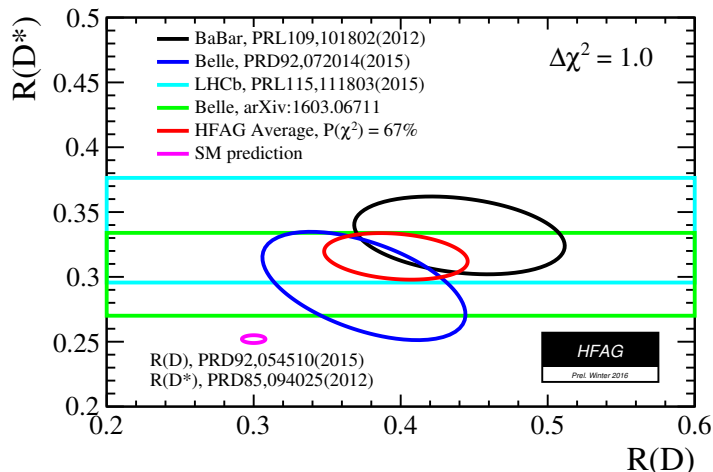
Fig. 1: Measured values and SM prediction of $R(D)$ and $R(D^*)$ [5]

clean: only two B mesons are produced and their initial energy is very well known. This allows us to fully reconstruct everything that happened inside the detector which is exceptionally useful in the case of making time–dependent CPV measurements. The ability to look at higher order decays makes us sensitive to particles with masses above those that can be produced directly at the colliders energy. This opens the door to a whole range of NP particle searches. Additionally, the clean environment allows us to look for invisible final states.

In addition to an upgrade of the hardware, the analysis software framework is also undergoing a major upgrade. The new framework, called the Belle AnalysiS Framework 2 (basf2), has been rewritten mostly from scratch with an emphasis on efficient use of resources and collaboration wide consistency. Making use of a central repository of common analysis modules, basf2 manages the processing of data and interaction with a central data store. The fact that each physics event is independent also allows for trivial parallelisation, either across a single machine's cores or multiple machines in a batch system.

2 SuperKEKB

The Belle II detector experiment is based at the Japanese High-Energy Accelerator Research Organisation (KEK) in Tsukuba, Japan. It will use SuperKEKB (Fig. 2), the upgraded KEKB electron–positron collider. SuperKEKB is an asymmetric e^+e^- collider with a 7 GeV electron high energy ring (HER) and a 4 GeV positron low energy ring (LER) inside a ~ 3 km circumference tunnel which has been reused from KEKB. The energies are selected such that they are at the $\Upsilon(4S)$ resonance, which is at almost exactly double the B meson rest mass. This results in a very high production rate of B meson pairs which are essentially at rest in the centre-of-mass (CoM) frame. The key changes made from KEKB are the so called Nano–Beam scheme which will squeeze the electron bunches and increase the instantaneous luminosity, and a change in the beam energies from 8 and 3.5 GeV to reduce emittance. The Nano–Beam scheme squeezes the electron bunches by minimizing the longitudinal size of the interaction point (IP) overlap region to effectively limit the minimum value of the beta function via the hourglass effect. The resulting Lorentz boost factor of the CoM system will be $\gamma = 0.28$, two thirds of that in Belle.

SuperKEKB is expected to achieve a peak instantaneous luminosity of 8×10^{35} cm^{-2}s^{-1} (Belle achieved: 2.11×10^{34} cm^{-2}s^{-1}). Over the six year lifetime of the experiment this will result in a total integrated luminosity of 50 ab^{-1} (Belle: 1 ab^{-1}). The projected luminosity profile is shown in Fig. 3, from which we expect roughly 55×10^9 $B\bar{B}$ events, 186×10^9 $q\bar{q}$ hadronisation events (the main source of background), and 46×10^9 $\tau^+\tau^-$ events.
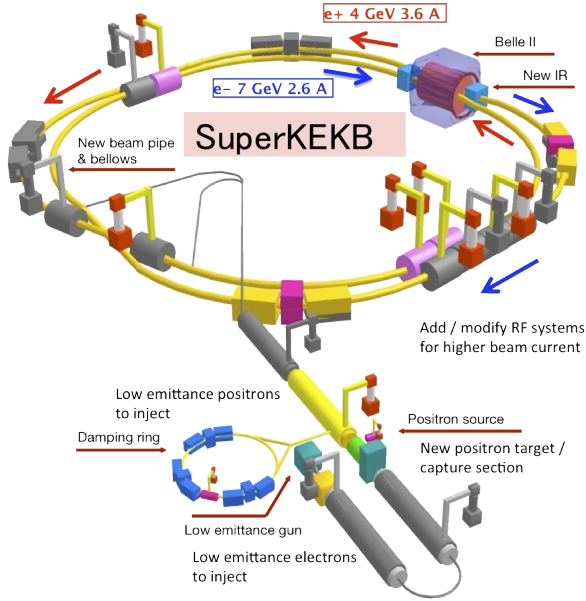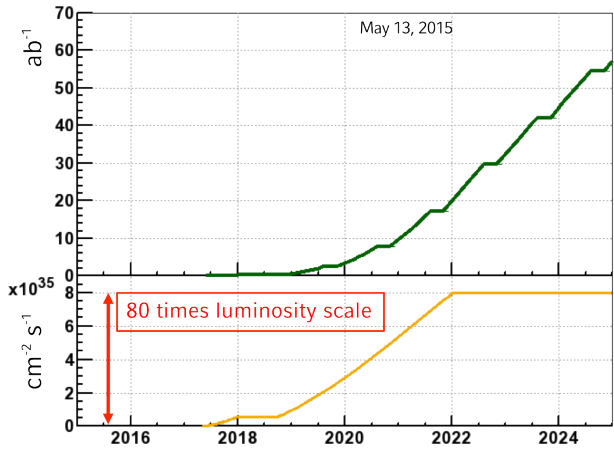
Fig. 2: The SuperKEKB accelerator.

Fig. 3: Instantaneous and integrated luminosity projections for SuperKEKB.

3 The Belle II Detector

The Belle II detector is the centrepiece of the experiment. It is a 7×7.5 m full–solid–angle detector with many sub-detector layers surrounding the interaction point. The detector is based on the design of the predecessor Belle detector with the goal of maintaining the performance of the Belle detector in the presence of considerably higher background levels. A sketch of the Belle II detector is shown in Fig. 4. The detector is comprised of the following sub-detectors which will be described in detail in the next sections: Vertex detector (VXD), Central drift chamber (CDC), Particle identification (PID) detector, Electromagnetic calorimeter (ECL), K–Long and Muon detector (KLM). The key changes from the Belle detector are [3]:

– The beam pipe radius at the interaction point has been reduced from 15 to 10 mm allowing the vertex detector to be closer to the interaction point. This allows for more precise vertex reconstruction but also increases the backgrounds faced by the innermost layers which increases roughly with the inverse square of the radius.

– The inner two layers of the silicon strip detector, immediately outside the beam pipe, will be replaced with a two–layer pixel detector to provide high precision track position measurements. This will provide excellent spatial resolution complementary to the fast timing resolution of the silicon strip detectors, while also being radiation hard enough to handle the high occupancy close to the beam pipe.

– The remaining silicon strip detector will be extended to larger radius. This will allow for a higher quality of track reconstruction and occupies the full volume inside the CDC.

– The CDC will have a larger volume and smaller cell sizes than in Belle, resulting in a much better momentum and dE/dx resolution.

– Particle identification will be performed by entirely new devices using Čerenkov imaging with faster read–outs than in Belle. The upgrade is necessary to cope with a higher background environment and also improves the K/π separation.

– The end–cap scintillator crystals, CsI(Tl), in the ECL will be replaced with faster, more radiation tolerant pure CsI crystals, and new electronics will be used. This allows the ECL to be resistant to the radiation induced degradation and pile-up noise caused by the increased luminosity.

– The end–cap and inner layers of the KLM are to be replaced with scintillators to allow for a shorter dead time and shielding from neutrons and other ambient backgrounds.
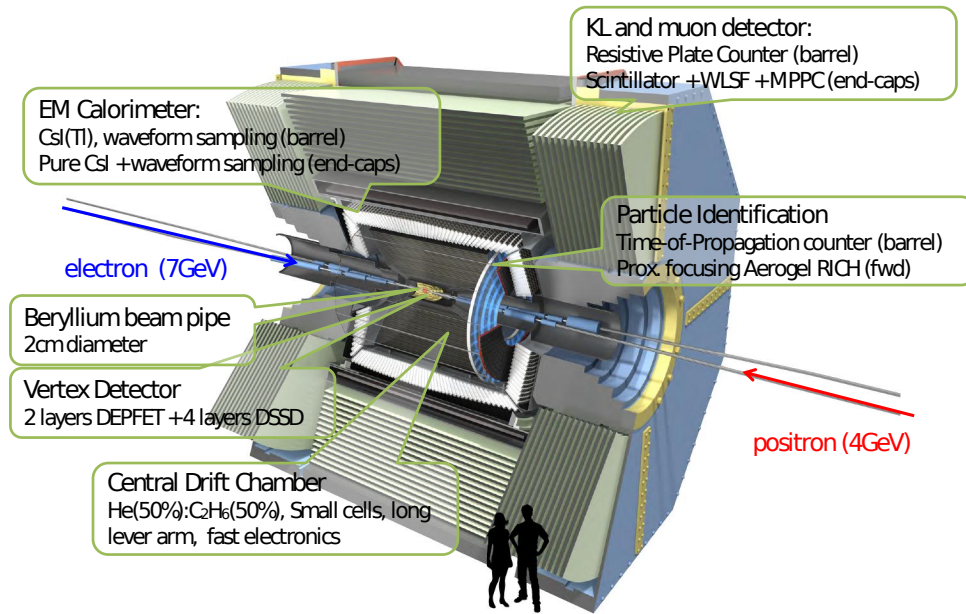

Fig. 4: Cross–section of planned Belle II detector [8]

3.1 Vertex Detector

The vertex detection module is comprised of two sub-detectors: a pixel detector (PXD) and a silicon vertex detector (SVD). The PXD contains two layers of the DEPleted p–channel Field Effect Transistor (DEPFET). The SVD is made of four layers of Double Sided Strip Detectors (DSSD). The primary purpose of the vertex detection system is to measure the vertices of the two B meson decays for mixing–induced CPV measurements and the vertices of D meson and τ lepton decays. Given the lower CoM boost in SuperKEKB, the two B meson decay vertices will have a smaller separation than in Belle. Despite this, the smaller beam pipe width at the interaction region and the larger radius of the SVD will allow Belle II to have as good as or better vertexing performance than Belle.

3.1.1 Pixel Detector

At the high luminosity expected the detector components closest to the beam pipe will experience incredibly high hit rates coming from beam–related backgrounds (e.g. Touschek effect) and low–momentum–transfer QED processes (e.g. photon–photon interactions). The beam pipe radius at the IP is only 10 mm, and since the background increases roughly with the inverse square of the radius strip detectors can no longer be used for the innermost layer due to the large fraction of channels hit in each triggered event (i.e. larger occupancy). Thus pixel detectors, which have a larger number of channels, will be used for the two innermost layers of the vertex detector. The two layers of the PXD will be at radii 14 mm and 22 mm from the beam line. Pixel detectors have been successfully used in detectors at the LHC [9] [10], however the lower energy of SuperKEKB means that thinner sensors need to be used. The DEPFET technology will allow for sensors as thin as 50 microns which only require air cooling and that are sufficiently radiation hard. A schematic of the DEPFET sensor layout in the PXD can be seen in Fig. 5, note the ladder structure to ensure full coverage of the acceptance region. The pixels, shown in Fig. 6, performs both detection and amplification in one [3] [11]. The inner layer of the pixel detector will contain

8 modules (ladders) with a total of 3.072 M pixels. The outer layer will have 12 modules with a total 4.608 M pixels. Two of the PXD modules have been produced and undergone beam tests along with the SVD. The remaining modules are still in production with ongoing lithography and quality tests.
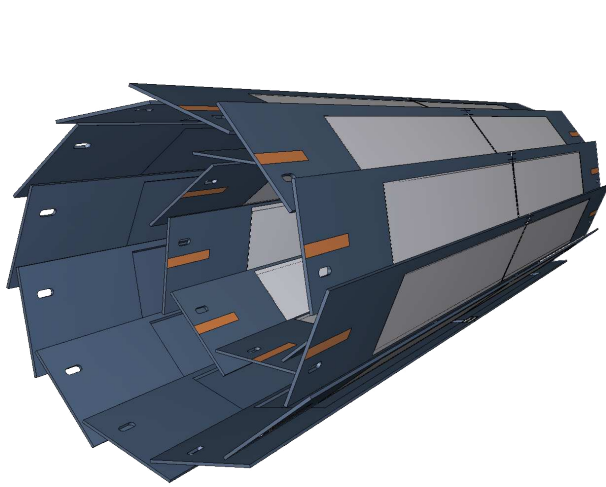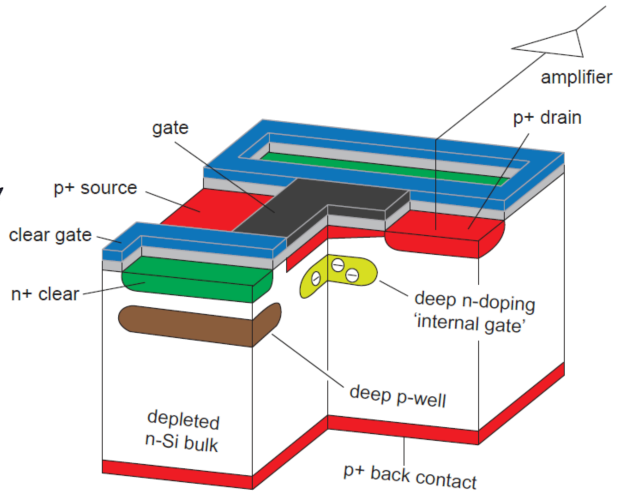

Fig. 5: Ladder structure of pixel detector modules.

Fig. 6: Single DEPFET pixel components.

3.1.2 Silicon Vertex Detector

The SVD comprises the outer four layers of the vertex detection sub-detector at radii 38, 80, 115, 140 mm [12]. Comparing this with Belle, which had its outermost SVD layer at a radius of only 88 mm, the reconstruction efficiency of low–momentum particles and long–lived particles is expected to improve significantly. The SVD in Belle II will cover the full detector acceptance range of $17° < \theta < 150°$. The hit occupancy will be required to be less than 10% to ensure that hits in the SVD are correctly associated with tracks in the CDC. The higher beam current and luminosity will increase the required trigger rate to 30 kHz, compared to the $\sim 1kHz$ trigger rate required in Belle.

Three sizes of double–sided silicon microstrip detectors (DSSDs) are used for the outer, inner, and forward sections. Each DSSD will be 123 mm long, and 300 or 320 μm thick. The DSSDs on the innermost SVD layer (layer 3 of the VXD) will have a width of 38 mm while the remaining layers will have DSSDs which are 58 mm wide. The DSSDs provide excellent timing resolution ($\sim$ 2-3 ns) which will complement the excellent spatial resolution of the PXD. The SVD ladders are still in construction; however, recently a test setup of the SVD and PXD (VXD mock–up) underwent beam tests at The Deutsches Elektronen-Synchrotron (DESY) in Hamburg, Germany, to measure the spatial resolution and hit efficiency.

3.2 Central Drift Chamber

The CDC is the main tracker for charged particles in Belle II. It contains 14,336 sense wires and 42,240 field wires, while a superconducting solenoid coil surrounding the ECL supplies a 1.5 T magnetic field. The CDC has three key roles in Belle II: to reconstruct charged tracks with high momentum precision, to provide particle identification information using measurements of energy loss (e.g. for identifying low momentum tracks which do not reach the PID detector), and to provide efficient and reliable trigger signals for charged particles. Given the success of the CDC design in Belle the same design structure will be used in Belle II. A comparison of the major parameters in Belle and Belle II can be seen in Table 1.

The key changes to the CDC design are:

- New readout electronics will be used to handle the higher trigger rates with less deadtime.
- The CDC inner radius and outer radii will be changed to avoid high backgrounds near the IP and to make room for the new, larger VXD.
- The CDC will generate 3D trigger information using a trigger in the z-direction.

The CDC has recently undergone cosmic ray testing in partnership with the barrel PID sub-detector and is now being calibrated and moved into its final position.

Table 1: Comparison of main CDC parameters in Belle and Belle II.

	Belle	Belle II
Radius of inner cylinder (mm)	77	160
Radius of outer cylinder (mm)	880	1130
Radius of innermost sense wire (mm)	88	168
Radius of outermost sense wire (mm)	863	1111.4
Number of layers	50	56
Number of sense wires	8,400	14,336
Gas	$He - C_2H_6$	$He - C_2H_6$
Diameter of sense wire (μm)	30	30

3.3 Particle Identification

The PID sub-detector is completely new in Belle II and contains two components: a Time Of Propagation (TOP) detector and an Aerogel Ring Imaging Čerenkov (ARICH) detector. The TOP detector is used for particle identification in the barrel region of Belle II, while the ARICH detector performs particle identification in the forward end–cap region.

3.3.1 Time of Propagation Detector

The goal of the TOP detector is to improve K/π separation while coping with the increased backgrounds expected from SuperKEKB. Overall the TOP contains sixteen modules, each module comprised of: two 2.7 m long quartz bars, a spherical mirror on one end of the bars, and an expansion prism with an array of photo–detectors attached on the other. The setup of a single TOP module can be seen in Fig. 7. It will use micro–channel–plate photomultiplier tubes (MCP–PMTs) and waveform sampling electronics for high precision position and timing measurements. The Čerenkov ring is reconstructed in three–dimensions from the measured time and the $x - y$ position of the Čerenkov photon hits on the MCP–PMTs. TOP modules have been tested at SPring-8 at LEP in 2013 during beam tests and met the required timing resolution of $\sim O(100 \, \text{ps})$. The modules have been installed in Belle II and are undergoing background tests and timing calibration.

3.3.2 Aerogel Ring Imaging Čerenkov Detector

The ARICH detector will be used for particle identification in the forward end–cap. Each detector module contains two adjacent layers of aerogel ($20 + 20$ mm thick) separated by an expansion volume (200 mm) from an array of 420 Hybrid Avalanche Photo Detectors (HAPD). The two layers of aerogel have differing refractive indices to provide overlapping of the Čerenkov rings for a better photon yield. The focusing of the ARICH has been optimized to seperate kaon Čerenkov photons from pion Čherenkov photons across most of their momentum range, while also discriminating between pions, muons, and

electrons in the momentum range below 1 GeV/c. An example of how kaons and pions can be discriminated between is shown in Fig. 8. The aerogel crystal installation will be completed in September 2016, with full system testing sheduled for January 2017.
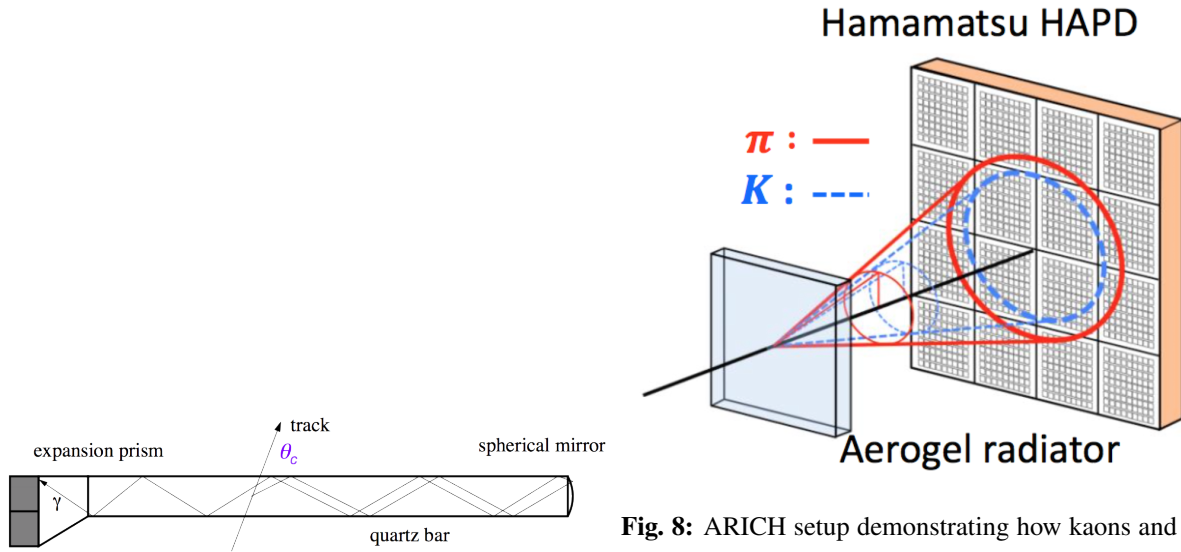

Fig. 8: ARICH setup demonstrating how kaons and pions with the same momentum can be dicriminated between [13].

Fig. 7: Single TOP detector module components [13].

3.4 Electromagnetic Calorimeter

Following the success of the ECL in Belle, the Belle II ECL will follow the same design with upgrades to handle the higher backgrounds expected. The CsI(Tl) barrel crystals from Belle will be reused while in the end–cap they will be replaced with pure CsI crystals [14]. New electronics will also be used with bias filtering and waveform sampling for faster readouts. The coverage of the ECL will be $12.4° < \theta < 155.1°$, excluding two $\sim 1°$ gaps where the barrel and end–caps join. The key roles of the ECL will be to: detect photons with precision measurements, identify electrons, take on–line and off–line luminosity measurements, and help detect K_L^0 together with the KLM. Performance studies are currently being carried out on the new crystals, whilst the electronics have been installed and tested.

3.5 K_L and μ Detector

The KLM in Belle II will be made of alternating layers of 470 mm thick iron plates and detector components. The resistive plate chambers (RPCs) that were used throughout the entire Belle KLM to detect charged particles will not be efficient enough to handle the ambient hit rate expected in the Belle II end–caps and barrel inner–layers. Instead scintillators will be used in the entire end–cap and first two layers of the barrel section, with RPCs used for the remaining barrel layers. In the barrel there are 15 detector components and 14 iron plates. In the forward (backward) end–cap there are 14 (12) detector layers and 14 (12) iron plates. The iron plates also serves as a magnetic return flux for the solenoid and provide interaction material in which K_L^0 mesons can shower hadronically. The total coverage of the KLM (barrel + end–caps) will be $20° < \theta < 155°$. The barrel KLM was the first sub-detector to be installed in Belle II in 2013. The end–caps were installed in 2014. The end–cap hardware is finished and undergoing software geometry and alignment calibration, while the final barrel components are being installed and tested. Cosmic ray testing for the entire KLM is ongoing.

4 Milestones

Currently the Belle II collaboration has ~ 650 members from 99 institutes in 22 countries, and is on track to begin data taking by the end of 2018. The first electrons circulated SuperKEKB at the beginning of 2016 as part of the first of three major phases in the Belle II experiment schedule. Phase 1, which ran from February until June this year, involved the beam commissioning with the dedicated detector BEAST II used to take beam background measurements. Phase 2 is currently scheduled to begin in December 2017 when SuperKEKB will begin to tune the collisions. At this point the Belle II detector, without the VXD, will be in place taking measurements. The start of the full physics run, the so-called phase 3, is set to begin in November 2018, at which point the completed Belle II detector will be installed and fully operational.

5 Summary

Having proved themselves as invaluable tools in the precision flavour frontier, B–factories offer a unique angle from which to probe the Standard Model and beyond. The Belle II experiment will play an important role in new physics searches as a complement to searches at other experiments. The upgraded luminosity of SuperKEKB will provide the high statistics needed for precision measurements, while improvements in all sub-detectors from its predecessor Belle will allow the Belle II detector to record clean data in the presence of the expected high backgrounds. The construction and testing of hardware and software components are progressing well, with the Belle II experiment set to begin taking data in 2018, with the aim of collecting a total of $50\ ab^{-1}$ by the end of 2024.

References

[1] M. Kobayashi and T. Maskawa, CP Violation in the Renormalizable Theory of Weak Interaction, *Prog. Theor. Phys.* **49** (1973) 652. https://doi.org/10.1143/PTP.49.652

[2] S. K. Choi *et al.* [Belle Collaboration], Observation of a resonance-like structure in the pi+- psi-prime mass distribution in exclusive B —> K pi+- psi-prime decays, *Phys. Rev. Lett.* **100** (2008) 142001. https://doi.org/10.1103/PhysRevLett.100.142001

[3] T. Abe *et al.* [Belle-II Collaboration], Belle II Technical Design Report. [arXiv:1011.0352 [physics.ins-det]].

[4] A. Abdesselam *et al.* [Belle Collaboration], Measurement of the branching ratio of $\bar{B}^0 \to D^{*+}\tau^-\bar{\nu}_\tau$ relative to $\bar{B}^0 \to D^{*+}\ell^-\bar{\nu}_\ell$ decays with a semileptonic tagging method. [arXiv:1603.06711 [hep-ex]].

[5] Heavy Flavor Averaging Group (HFAG) Winter 2016, `http://www.slac.stanford.edu/xorg/hfag/semi/winter16/winter16_dtaunu.html`.

[6] P. Urquijo, Physics prospects at the Belle II experiment, *Nucl. Part. Phys. Proc.* **263-264** (2015) 15. https://doi.org/10.1016/j.nuclphysbps.2015.04.004

[7] R. Fleischer, Theoretical prospects for B physics, PoS FPCP **2015** (2015) 002. [arXiv:1509.00601 [hep-ph]].

[8] Belle II website, `https://www.belle2.org`.

[9] J. Karancsi [CMS Collaboration], Operational Experience with the CMS Pixel Detector, *JINST* **10** (2015) C05016. https://doi.org/10.1088/1748-0221/10/05/C05016. [arXiv:1411.4185 [physics.ins-det]].

[10] Y. Takubo [ATLAS Collaboration], The Pixel Detector of the ATLAS experiment for the Run2 at the Large Hadron Collider, *JINST* **10** (2015) C02001. https://doi.org/10.1088/1748-0221/10/02/C02001, 10.1088/1748-0221/10/12/C12001. [arXiv:1411.5338 [physics.ins-det]].

[11] J. Schieck [DEPFET Collaboration], DEPFET pixels as a vertex detector for the Belle II experiment, *Nucl. Instrum. Meth. A* **732** (2013) 160. https://doi.org/10.1016/j.nima.2013.05.054

[12] G. B. Mohanty, Belle II Silicon Vertex Detector, *Nucl. Instrum. Meth. A* **831** (2016) 80. http://doi.org/10.1016/j.nima.2016.04.013. [arXiv:1511.06197 [physics.ins-det]].

[13] B. Wang [Belle-II Collaboration], The Belle II Experiment and SuperKEKB Upgrade, [arXiv:1511.09434 [physics.ins-det]].

[14] B. Shwarz [BELLE II calorimeter group Collaboration], Electromagnetic Calorimeter of the Belle II detector, PoS PhotoDet **2015** (2016) 051.